Laboratory scale tests of a floating tidal turbine

S. Walker
College of Engineering, Mathematics and Physical Sciences, University of Exeter, Penryn, UK

L. Cappietti, I. Simonetti
LABIMA, Dept. of Civil and Environmental Engineering, University of Florence, Florence, Italy
A-MARE Joint Laboratory

A. Esposito
AM3 Spin-off s.r.l., Italy
A-MARE Joint Laboratory

ABSTRACT: Tidal stream energy has great potential to reduce the greenhouse gas emissions of electricity supply, but development has been slow, in part due to high costs and challenging engineering required to operate in the marine environment. Floating support structures may be able to help reduce these costs. A laboratory study comparing the performance of a turbine mounted on fixed and floating support structures was used to investigate this potential. Realistic flow and wave cases were established from two installation sites. The turbine was found to generate greater power when mounted on a floating structure across all wave and flow cases, and the support structure experienced less strain. In both cases, the ability of the floating structure to move in response to wave action is believed to be the key factor. Floating support structures are not without challenges, but may offer a route to lower cost tidal stream turbine installations.

1 INTRODUCTION

1.1 *Tidal stream energy*

Tidal stream energy has long been suggested as a major future contributor to the energy requirements of many countries, particularly in Europe and the Americas where large tidal ranges occur. Whereas most other forms of renewable energy (e.g. wind and wave) are ultimately driven by solar power, tidal is alone in being gravitationally driven. This gives it a unique advantage, in that it does not suffer from the intermittency of many other renewable energy sources. This intermittency is a major obstacle in the process of electricity supply decarbonisation, since it requires renewable energy sources to be “backed-up” by reliable sources (commonly fossil fuels) to allow continuous power during periods of low renewable generation. Moreover, the intermittency and the related high time variability of available energy flux impact in the sizing of the devices’ rated power and so it in turns impacts in the cost-benefit balance of renewable energies devices.

Since tidal stream energy offers the advantages of renewable energy without the disadvantage of intermittency, it seems surprising that the technology has not been more widely adopted. Indeed, twelve years after the first commercial device was deployed, there are still only a handful of tidal turbines operating around the world. The underlying reasons for this slow adoption are primarily related to the complex and expensive engineering challenges which must be addressed to install and operate tidal stream turbines. Although similar challenges exist in all renewable energy fields, the tidal environment is perhaps especially challenging. Environments in which tidal stream turbines are likely to be installed (commonly channels between landmasses) are inherently highly energetic environments, and require heavily-engineered structures. Potential installation sites can experience flow speeds of up to 4 m/s and waves of 6 m in height, or even greater during storm conditions. Though much greater flow speeds are experienced by wind turbines, the relative density of air and water means that tidal turbines experience forces far in excess of those ever experiences by wind turbines. Designing a structure to survive these conditions, and to provide consistent and reliable energy generation for a design lifetime of perhaps 25 years is a major engineering challenge. The cost of addressing this challenge is one of the reasons that may have limited the adoption of tidal stream energy to date.

1.2 *Fixed vs Floating*

A classic paradox helps suggest an alternative to the common seabed-mounted tidal turbine design. The paradox asks "What happens when the unstoppable force meets the immovable object?". Superman (DC Comics, 2005) suggests that the answer may be the surrender of one party. When designing a fixed tidal stream turbine, the structural engineer aims to design a structure such that it is the unstoppable force

which surrenders: the flow is diverted around the structure of the turbine, causing an increase in pressure in the surrounding area but leaving the structure undamaged. However, in order to ensure that this is the case, the fixed support structure and foundation system must be designed to survive the worst combined flow and wave conditions expected during the turbine's lifetime, or risk a catastrophic failure. This is achievable, but requires a high level of structural redundancy, which has material, energy and financial costs. If the turbine were instead attached to a floating structure, which was able to move with the action of flow and waves, it would be able to surrender to the flow without failure, and would therefore not require the same level of structural redundancy. However, the fact that the structure would require mooring introduces complexity not present in the fixed case, which itself may lead to additional cost, material and energy use.

This work aims to assess whether a tidal stream turbine mounted on a floating support structure is able to achieve the same performance as a turbine mounted on a fixed seabed support structure, within realistic wave and flow condition cases.

2 METHOD

In order to carry out this comparison, a scale model tidal stream turbine was tested in the experimental wave-current flume at LABIMA (Florence University) in two layouts: Firstly mounted on a fixed support structure, and secondly mounted on a floating support structure. Flow and wave cases were developed from realistic locations in Scotland and Italy.

2.1 *Locations*

Two real sites were used to generate the input data for this study, one in the Messina Strait in the Mediterranean Sea, and one in the Sound of Islay in the North Atlantic. To generate realistic site data, we first selected feasible tidal turbine installation locations. These locations were chosen as they represent the extremes of potential tidal location sites. While tidal velocities at both sites are sufficient to make the sites potentially suitable for economic power extraction, the Sound of Islay site is a very energetic site, while the Messina Strait site is in a calmer location.

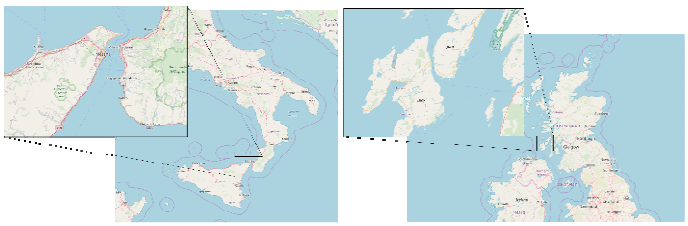

Figure 1: Locations used for the generation of realistic flow cases. Messina Strait (l) and Sound of Islay (r).

The Messina Strait is a 5km wide channel between the Italian mainland and the island of Sicily, at the meeting of the Ionian Sea to the south and the Tyrrhenian Sea to the north, and is perhaps one of the most suitable sites for tidal power generation in the Mediterranean. The deepest point of the channel is 250m deep, and tidal velocities reach 2.5m/s (Cucco, 2016). Figure 1 (l) shows the location of the strait and the location used in this study.

Maximum ebb and flow values in the Messina Strait occur at different locations (Longhitano, 2018), so the location with the greatest mean absolute value of flow velocity was selected. The selected location is at a latitude of 38.23°N and longitude 15.62°E.

The Sound of Islay is a channel between the islands of Islay and Jura, off the west coast of Scotland. The channel is approximately 1km wide, and 198m deep at its deepest point. The channel is known for high tidal velocities, with a maximum of around 3.7m/s. The location selected for use in this study lies at latitude 55.85°N and longitude of 6.10°W. Figure 1 (r) shows the location used in this study.

2.2 *Flow cases*

Both recorded and hindcast data was used to collect flow velocity and wave conditions for the two sites. Data from EMODnet (EMODnet, 2018) was used to provide bathymetric conditions and aid the scaling of the experiments. Tidal flow velocity conditions were classified using data from the Copernicus Marine Environment Monitoring Service (Copernicus, 2017, Copernicus, 2017b) This data was recorded at a frequency of 30 minutes for the full year of 2017.

Wave data for the Messina Strait case was taken from the wave hindcasting based on the Wavewatch III model by Pelli, 2016. It suggests that this location experiences similar wave conditions to other Mediterranean areas. So, in the perspective of the aims of the present work, also the data from the Italian Wave Network (Vicinanza, 2009) buoys can be used. It provides wave measurements recorded for a 30-minute period at a three-hour frequency between 1/7/1989 and 31/12/2007.

Wave data for the Sound of Islay case was taken from the DHI MetOcean Data Portal (MetOcean, 2017). Data was recorded by the NASA Jason-1 satellite with temporal resolution of around 2 seconds. Data recorded between 15/3/2016 and 15/3/2017 was used in this study.

At the two locations, flow velocity data was classified into three categories: Benign, moderate, and extreme, representing the 80^{th}, 90^{th} and 95^{th} percentiles of flow velocity data respectively. It was found that benign and moderate conditions in the

Sound of Islay case corresponded almost exactly to moderate and extreme cases in the Messina Strait case. Two flow velocity cases were therefore selected: *flow case 1*, with a flow velocity of 1.3m/s (benign in the Sound of Islay case and moderate in the Messina Strait case) and *flow case 2*, with a flow velocity of 1.7m/s (moderate for the Sound of Islay and extreme for the Messina Strait).

Previous work (Walker, 2019) highlighted the importance of wave period, so it was decided to consider three different wave periods for the same wave height. Wave periods of 7.2 s, 9.0 s and 10.8 s were selected (corresponding to benign, moderate and extreme wave periods as measured in the Messina Strait), with a constant wave height of 4.0m. A summary of the cases selected is shown in Table 1. In all cases, waves propagate with flow.

Table 1. Flow and wave cases studied.

	Flow conditions	Wave conditions	
	Velocity (m/s)	Height (m)	Period (s)
Flow case 1:			
Wave case 1	1.3	4.0	7.2
Wave case 2	1.3	4.0	9.0
Wave case 3	1.3	4.0	10.8
Flow case 2:			
Wave case 1	1.7	4.0	7.2
Wave case 2	1.7	4.0	9.0
Wave case 3	1.7	4.0	10.8

2.3 *Water channel*

The resulting case scenarios were then scaled 1:81 to the water channel size and used to establish test cases during the experimental campaign.

The Wave-Current Flume at LABIMA, University of Florence, is 37 m in length and 800 mm wide. A water depth of 300 mm was used for all tests in this study. A recirculating pump is installed in a pipe manifold of 250 mm diameter and controlled by a frequency modulating controller (model Danfoss VLT). The wave maker is a bespoke LABIMA system capable of producing waves of up to 0.35 m with period about 3s. Wave height were measured using ultrasonic wave gauges (model Honeywell 943-F4V-2D-1C0-330E). Four such gauges were used, installed at approximately one third and two thirds of the distance across the channel (250 mm from the channel walls in each case), at 420 mm upstream and 430 mm downstream of the turbine installation location. Flow rate was measured by a magnetic flow meter (model Danfoss MAGFLO MAG3100W). The real velocities described in the previous section (Table 1) give velocities and bulk flow rates through the channel of 0.16 m/s and 37.5 l/s and 0.21 m/s and 50 l/s respectively.

It is well known that the upstream turbulence intensity plays a key role in the response of horizontal axis turbine, and it may affect both blade loading and power extraction (Blackmore, 2014, Blackmore, 2016, Ahmadi, 2019). For this reason, prior to testing, the channel was characterised in order to capture flow profiles and turbulence data for the cases to be tested. Profiles were captured using a Nortek Vectrino Acoustic Doppler Velocimeter at the turbine installation location for each of the wave and flow cases subsequently used to test the turbine.

In order to ensure a realistic level of turbulence in the channel, turbulence-generating structures were installed upstream and downstream of the turbine installation location (Figure 3). A combination of blocks and mesh were used. Cubic stone blocks of 120 mm width and height were installed with a cross-channel separation of 150 mm and a streamwise separation of 200 mm between rows. Alternating rows of two and three blocks were used, covering a total distance of 2.4 m between 7.7 m and 10.1 m upstream and 7.9 m and 10.3 m downstream of the turbine installation location (Figure 3). (NB: downstream blocks were used as turbulence-generating structures for experiments to investigate the effect of reverse flow, which are not described here) Two stainless steel meshes of 12 mm grid size was installed across the channel and over its full depth, at a distance of 6.5 m upstream and 6.7 m downstream of the turbine installation location. An absorbing structure was placed at the end of the channel to diffuse wave power and reduce reflection. This perforated steel structure was 2.4 m in length and reached across the channel, angled upwards from the base to above the height of the highest waves to be tested. The downstream turbulence-generating blocks and mesh used are illustrated in Figure 2.

Figure 2: Turbulence-generating mesh and blocks installed in the LABIMA water channel.

For the two flow velocity cases studied, mean streamwise turbulent intensities for cases without waves were between 4.9% and 6.2%. Profiles are illustrated in Figure 4. Details on the procedure

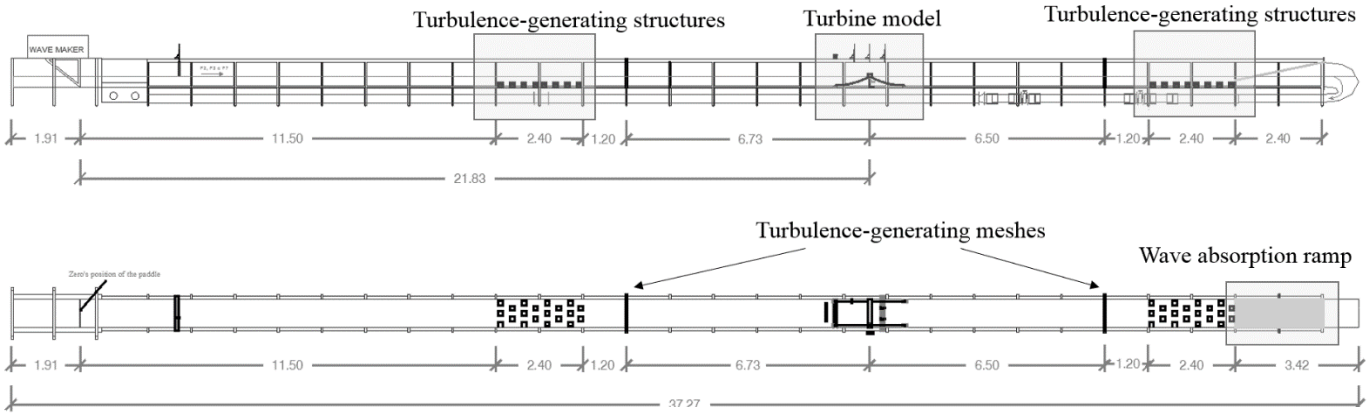

Figure 3: Wave-Current flume layout and turbine model position during tests at LABIMA.

adopted to calculate turbulent intensity from measured data can be found in (Walker, 2017). The addition of waves increased mean streamwise

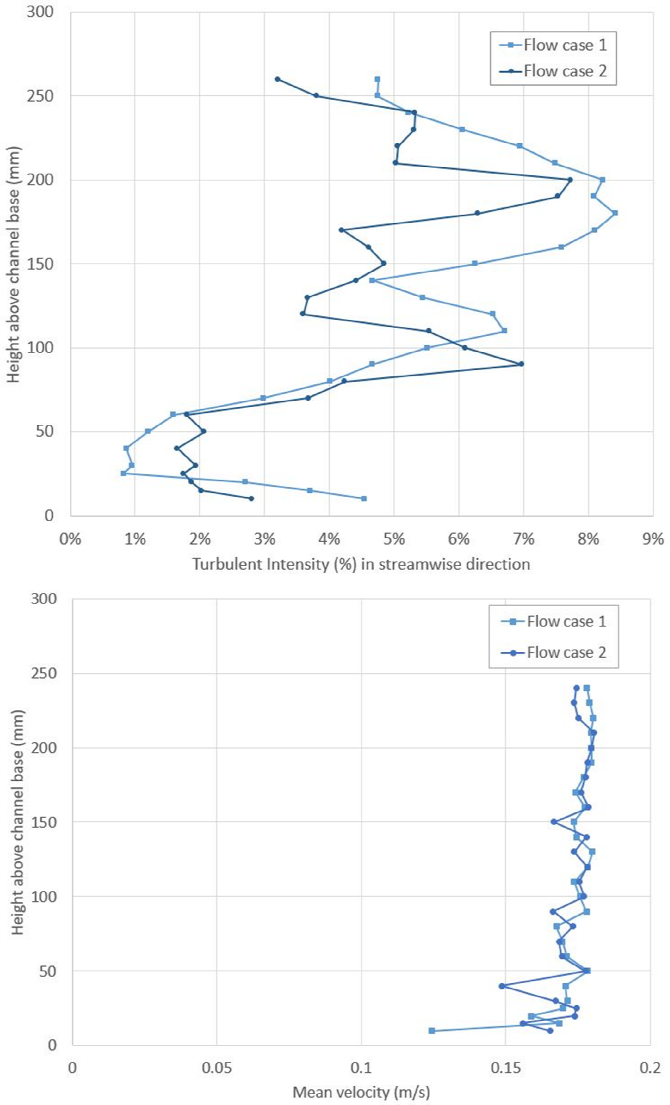

Figure 4: Turbulent intensity (top) and mean streamwise flow velocity (bottom) recorded in the LABIMA Wave-Current flume for flow cases 1 and 2.

turbulent intensity values to between 5% for low flow rate and 15% for high flow rate cases. This compares to real turbulence intensity of 12-13% recorded experimentally at a site with maximum flow velocity of 2.5 m/s (Milne, 1985).

2.4 *Turbine model*

The turbine model used in this study was a 1:81 scale three-blade horizontal axis turbine, representative of most commercial tidal turbine concepts, using Froude scaling. The blade profile was based on that of a commercial design and was manufactured in polyacrylate at the University of Sheffield Department of Applied Inkjet Printing. The turbine blades each measure 100 mm from root to tip, with a 12° degree root-tip twist, a tip chord of 8 mm and a root chord of 26 mm. The blades were mounted on a nacelle, which was itself fixed to the 27.5 mm diameter turbine generator. No gearbox or other power transfer mechanisms were used.

For the fixed support structure cases, a simple 8 mm diameter post design without a complex support base, tripod or other fixing arrangement was used. This design was chosen to allow the measurement of structural deflection on a homogeneous support structure. The turbine and support structure were mounted on a steel base of 200 mm x 200 mm and 7 mm thickness, designed to hold the turbine in position without a requirement to fix it to the base of the channel. The support structure was 117 mm in length from the base to the generator, meaning that the centre of the nacelle was 138 mm above the channel base. The turbine is shown in Figure 5.

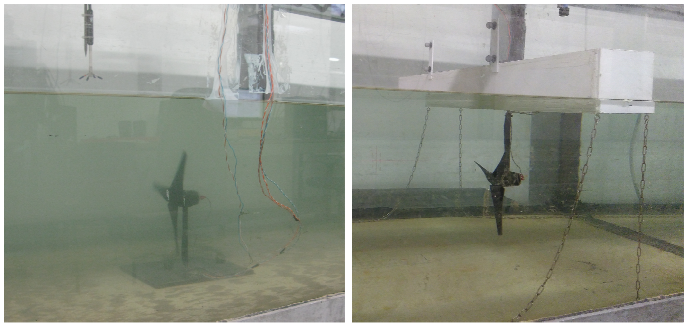

Figure 5: Turbine mounted on fixed (l) and floating (r) support structures

In floating support structure cases, the turbine was mounted on the same support structure, but was

inverted and mounted to the underneath of a floating structure. The size, volume and weight of the floating structure are representative of a prototype under design as a multipurpose structure, i.e. not just as turbine support structure only, in order to sharing the construction costs and producing renewable energy. The floating structure was 750 mm wide, with a cross section of 70 mm height and 70 mm width. The structure was made from 3 mm thick polystyrene sheet and was filled with cured polyurethane foam. The structure was moored using 950 mm long chains of 1 mm stainless steel and mounted to hooks fixed to the channel base with streamwise separation of 1.6 m and cross-stream separation of 700 mm (two upstream of the turbine and two downstream, set 50 mm from the side of the channel). The turbine was mounted at the centre of the base of the floating structure. In the floating case with zero flow or waves, the centre of the turbine nacelle was mounted 131 mm below the base of the floating structure. With the turbine mounted, the structure floated with its base 15mm below the water surface, placing the nacelle centre at 146 mm below the water surface, or 154 mm above the channel base. The difference in hub height of 16mm between the two cases places the turbine blades in a slightly different flow region and may impact the relative power generation.

2.5 *Instrumentation*

In order to measure performance and structural deflection, the turbine was equipped with a generator and strain gauges. A small DC motor (model MFA RE-385) was used as a generator. The voltage and current produced by the generator was measured using the LABIMA Data Acquisition system, allowing power to be calculated. Since the key performance output of the turbine in this study is the relative power generation, generator output was not scaled or calibrated to rotational speed. Instead, generator voltage was used to give a direct comparison between cases.

Copper foil strain gauges (model BF350, 350Ω, coefficient of sensitivity 2.1) were mounted at the vertical centre of the support structure, 58.5 mm from the base of the turbine. One gauge was installed on the upstream-facing portion of the support structure, and another perpendicular to this on the side of the support structure. Gauges were installed in a half-bridge configuration, and were supplied with 5 V via the LABIMA data acquisition system and deflection recorded using the same system.

In order to correlate support structure deflection and strain gauge voltage output, strain gauges were calibrated using a load cell (model AEP transducers Type FJ). A rigid steel bar was fixed between the load cell and the centre of the nacelle, and the turbine was incrementally moved towards the load cell whilst recording both strain gauge and load cell outputs. Testing was repeated multiple times. A linear relationship between deflection and load was observed, with a slope of 0.59 N/mV.

2.6 *Test procedure*

Prior to each test, flow conditions were set by adjusting the motor controller to a predetermined frequency to give the required flow rate for each velocity. A period of time was allowed to ensure stable flow conditions, then the test was started. LABIMA uses a combined wave generation and data acquisition system and all measurement equipment was routed through this system, resulting in a single output file for each test. Each test began with a 10 second period without waves, followed by a 60 second period of wave generation, followed by a 30 second period without wave generation. An acquisition frequency of 200 Hz was used for the ultrasonic wave gauge and for the strain gauges.

The turbine rotation was not controlled in any way. Performance was observed for the fixed and floating cases in otherwise identical flow conditions, using identical generation equipment. The aim of this method was to allow the comparative performance of the turbine to be observed.

3 RESULTS

Turbine performance and support structure strain were measured for fixed and floating turbine support systems for two flow cases and three wave cases introduced previously, as well as two initial case without waves.

3.1 *No waves cases*

In the no waves cases, there was variation between the mean power generated by the turbine mounted on fixed and floating support structures. In *flow case 1*, mean power over the sample period for the turbine using the floating support structure was 13.3% greater than that using the fixed support structure for the same sample period. In *flow case 2*, the difference was 5.7%, with the floating structure. case still performing better. It is worth highlighting this difference in mean power generated can be, in principle, explained in terms of different local flow conditions taking place at the turbines' hub level. It may in turn be related to the slightly different turbine hub position, or the floater blockage effect. A detailed analysis of this hypothesis is presently under investigation and results will be published in a second article.

For both the fixed and floating support structures, strain in cases without waves was characterised by small variation over a consistent mean. In both *flow case 1* and *flow case 2*, the floating structure turbine

recorded a mean strain value 51% lower than that of the fixed support structure turbine.

In the floating case, both the mean strain and variation in strain were lower than in the fixed support case.

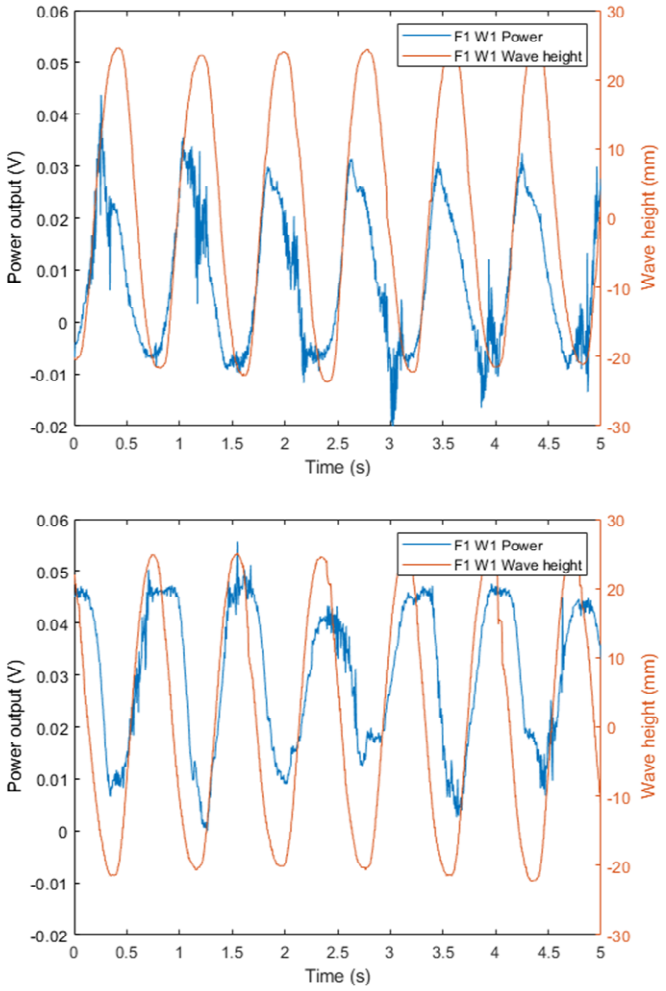

Figure 6: Power generation data for *flow case 1* (1.3 m/s) with *wave case 1* (4.0 m waves at 7.2 s period) for turbine mounted on a fixed (top) and floating (bottom) support structure

3.2 *Power Generation*

Basic power production patterns were similar in all cases with flow and waves. Broadly, mean power was found to increase with increasing flow rate, and the pattern of power production around the mean was found to vary with wave period. Maximum power generation occurred in all cases as the wave crest passed the turbine, and generation was at a minimum at the wave trough phase. However, there was a small variation between fixed support structure cases, where the peak generation was actually slightly before the wave maximum, and the floating support structure case, where the generation peak was slightly after the wave maximum. A comparison plot showing wave height relative to instantaneous power generation for *flow case 1* with *wave case 1* is shown in Figure 6.

As can also be seen in this data, the fixed support structure turbine power generation falls below zero during the period around the wave trough. This negative generation occurs when the turbine rotates backwards, which is caused by the effective reversal of the flow direction at the turbine blades due to negative wave-induced velocities during the passage of the trough. Notably, this effect is not seen in the comparable floating turbine case. This allows the floating support structure turbine to produce greater power over each wave cycle, and greater mean power generation in the longer term. This effect is seen in all combinations of wave and flow cases, though the effect is lower in cases with greater flow rate and longer wave periods. For comparison, a plot showing wave height relative to instantaneous power generation for such a case (*flow case 2* with *wave case 3*) is shown in Figure 7.

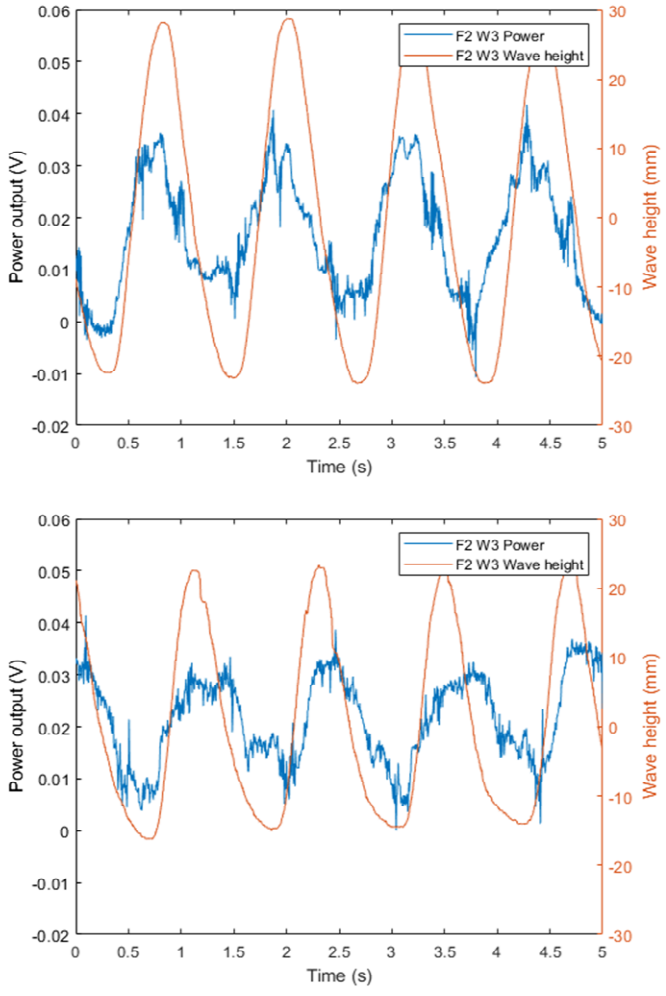

Figure 7: Power generation data for *flow case 2* (1.7 m/s) with *wave case 3* (4.0 m waves at 10.8 s period) for turbine mounted on a fixed (top) and floating (bottom) support structure.

In this case, the increased flow rate and longer wave period cause less flow reversal at the turbine blades, meaning that the turbine does not generate negative power during every wave (as shown in the second and third waves in Figure 7 (top)). Again, the turbine mounted on the floating structure does not

experience this effect at all, and thus power generation values are greater.

3.3 *Mean power generation*

The mean power generated over 10,000 samples (50 s) captured during wave generation for all cases is shown in Figure 8.

3.4 *Support structure strain*

Strain data was captured for all cases, using the strain gauge system described in Section 2. Strain data was recorded as deflection and converted to force via the calibration procedure described in Section 2.5. Data given here is the measured force on the support structure. The mean force recorded on the support structure in each flow and wave case for fixed and floating support structures is illustrated in Figure 9.

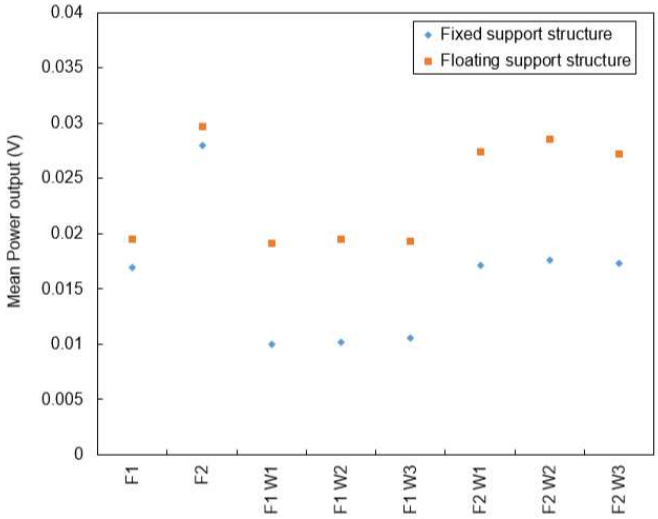

Figure 8: Mean power generation for turbine mounted on fixed and floating support structure in all flow and wave cases (as Table 1). Mean power generation for 10,000 samples during wave generation period (excl. F1 and F2 cases).

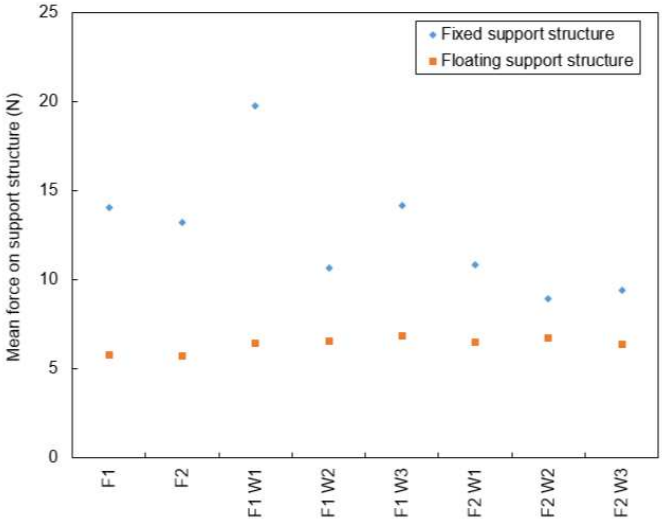

Figure 9: Mean support structure force experienced by fixed and floating support structures in all flow and wave cases (as per Table 1).

Mean force in the floating support structure case is between 5.6 N and 6.8 N, with minimum values recorded in the *flow case 1* and *flow case 2* tests without waves, and maximum values recorded in *flow case 1* with short period waves, and *flow case 2* with medium period waves. Even in the most benign cases, the fixed turbine support structure experienced forces greater than any of the floating turbine cases, with a minimum of 8.9 N recorded in under *flow case 2* with medium period waves.

However, the mean force data does not reveal the true forces applied to the support structures. Though the recording of strain data at high speed can be challenging, major differences were seen in the range of force values recorded in the fixed and floating cases. This was the case across flow and wave cases.

Using *flow case 1* and *wave case 1* as an example, Figure 10 shows recorded force data on the support

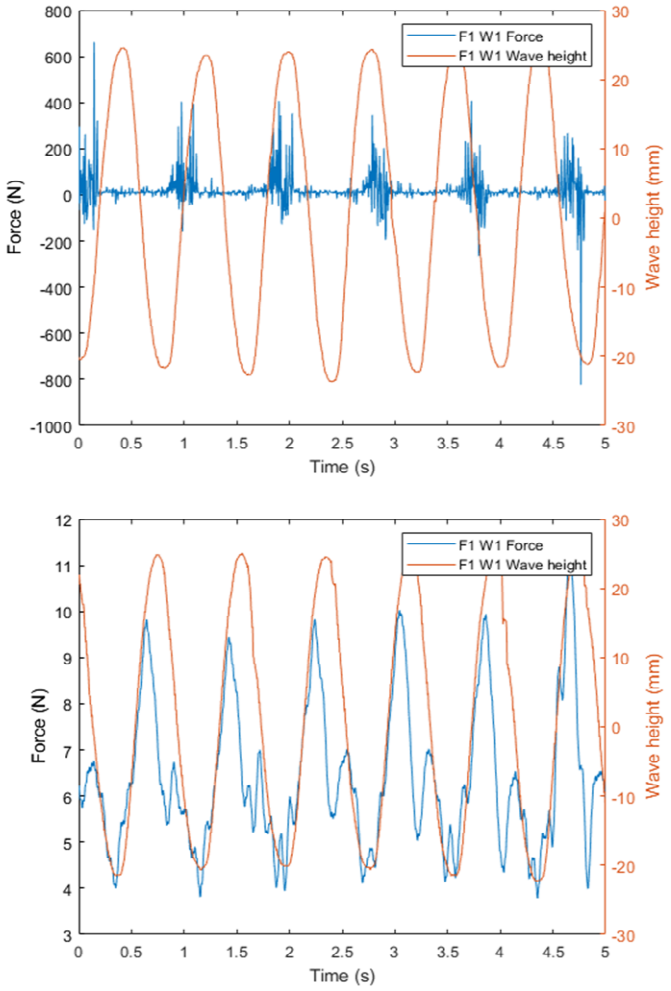

Figure 10: Support structure force *flow case 1* (1.3 m/s) with wave case 1 (4.0 m waves at 7.2 s period) for turbine mounted on a fixed (top) and floating (bottom) support structure.

structures for the fixed (top) and floating (bottom) cases. In the fixed case, the data shows values of the order of +700 N and -800 N. Whilst these individual sample values are extreme and appear to be caused by the instrument experiencing out-of-range values, it is clear that the fixed support structure experiences

a wide range and dramatic changes in applied force. Conversely, the floating support structure shows a clear pattern, with the greatest force experienced at the same time as the greatest change in wave height. The structure then relaxes as the wave peak passes, before experiencing a second force as the wave height again changes quickly. In the *flow case 1-wave case 1* fixed support structure case, a maximum range of 7 N was observed.

4 DISCUSSION

Across all cases tested, maximum power generation and minimum support structure strain occurred when a floating support structure was used instead of a fixed support structure.

The floating support structure allows better turbine performance, both in terms of power output (which is increased in comparison to the fixed structure) and strain (which is reduced). Power generation was greatest in *flow case 2*, as would be expected in this higher velocity flow. *Flow case* 2 without waves was also the case with the smallest difference in power generation between the fixed and floating support structures. After the introduction of waves, the floating support structure case still delivered power levels close to those without waves, whereas in the fixed support structure case, power levels were only around 60% of those without waves. This highlights the key finding of this work, which is that the use of a floating support structure appears to allow the turbine to be more resilient to waves than a fixed support structure. In cases with waves, the turbine with fixed support structure performs around 40% worse than the turbine mounted on the floating structure.

The fixed support structure is the most susceptible to forces due to waves, with greater values across all studied cases.

The reason for this difference in performance is believed to be related to the motion of the floating structure. This offers a clear explanation for the reduction in support structure strain, since the forces acting on the turbine in the floating case move the entire structure, whereas in the fixed case the same forces cause the structure to deflect, inducing stresses. In terms of our original paradox, the floating support structure allows the turbine to surrender, whereas the fixed structure remains immovable. The increase in power generation in the floating structure case relative to the fixed structure case appears to be related to the same effect. As each wave passes and causes an area of net lower velocity, the turbine is unable to escape this region and suffers a reduction in power generation. However, the motion of the floating support structure appears to move the turbine out of this region as the wave passes, meaning that it generates greater power than in the fixed case.

Findings of this work appear to support the suggestion that if a floating support structure is used, a turbine may generate comparable or greater power than if a fixed support structure is used, whilst experiencing less strain on the support structure. This means the support structure does not need to be as strong, and thus offers opportunities for savings in materials, transport and installation costs, and ultimately the potential for reduced lifetime energy cost.

5 CONCLUSIONS

We conclude that, for the flow and wave conditions simulated:

Floating support structures appear to experience less strain due to the action of waves, when compared to fixed support structures used in the same conditions.

Turbines mounted on floating support structures generate more power than those mounted on fixed support structures, when subjected to the same conditions.

A detailed analysis of the effect of floater blockage will be undertaken, and further tests over a wider range of conditions would be beneficial (for example in order to determine the limits of suitability of floating structures). Testing including assessment of mooring devices is critical, but initial findings suggest that floating support structures for tidal stream turbines may offer a route to cost reduction.

ACKNOWLEDGMENTS

Dr Stuart Walker was funded as part of the Tidal Stream Industry Energiser Project (TIGER), a European Union INTERREG V A France (Channel) England Research and Innovation Programme, which is co-financed by the European Regional Development Fund (ERDF).

Part of the present study was carried out within the EXTREMAL-FLOATER – MARINET2 project, which has received funding from the European Unions' Horizon 2020 research and innovation programme under grant agreement No. 731084.

REFERENCES

Ahmadi, M.H.B. 2019. Influence of upstream turbulence on the wake characteristics of a tidal stream turbine, *Renewable Energy*, Volume 132, pp. 989-997, ISSN 0960-1481.

Blackmore, T., Batten, W.M.J., Bahaj, A.S. , 2014.

Influence of turbulence on the wake of a marine current turbine simulator, *Philos. Trans. Royal Soci. A* 470 (2014), [Online]. Available: https://doi.org/10.1098/rspa.2014.0331.

Blackmore, T., Myers, L.E., Bahaj, A.S., 2016. Effects of turbulence on tidal turbines: Implications to performance, blade loads, and condition monitoring, *International Journal of Marine Energy*, Volume 14, 2016, pp. 1-26, ISSN 2214-1669.

E.U. Copernicus Marine Service Information: Copernicus Environment Monitoring Service Global Ocean 1/12° Physics Analysis and Forecast. Product GLOBAL_ANALYSIS_FORECAST_PHY_001_024. Longitude -8 to -1, latitute 55 to 59. Date 01/01/2017 00:30:00 to 31/21/2017 23:30:00

Copernicus Marine Service Information: Copernicus Environment Monitoring Service Global Ocean 1/12° Physics Analysis and Forecast. Product GLOBAL_ANALYSIS_FORECAST_PHY_001_024. Longitude 14 to 17, latitute 36 to 39. Date 01/01/2017 00:30:00 to 31/21/2017 23:30:00

Cucco, A., Quattrocchi, G., Olita, A., Fazioli, L., Ribotti, A., Sinerchia, M., Tedesco, C., Sorgente, R., 2016. Hydrodynamic modelling of coastal seas: the role of tidal dynamics in the Messina Strait, Western Mediterranean Sea. *Nat. Hazards Earth Syst. Sci*. 16, 1553–1569.

Morrison, G., Quietly, F., All-Star Superman, DC Comics 2005.

Bathymetric metadata and Digital Terrain Model data , EMODnet Bathymetry portal, 9th October 2018, [Online] Available: http://www.emodnet-bathymetry.eu

Longhitano, S. G., 2018. Between Scylla and Charybdis (pt 1): the sedimentary dynamics of the modern Messina Strait (central Mediterranean) as analogue to interpret the past. *Earth-Science Reviews* 185 pp. 259-287

DHI MetOcean Data Portal. Global Wind Speed, Wave Height and Wave Period, Satellite Altimeter Measurements. Geographical reference EPSG:4326 (WGS84). NASA Jason-1 satellite data via MetOcean Data Portal for 15/3/16 - 15/3/17.

Milne I. A., Sharma R. N., Flay R. G., Bickerton S. Characteristics of the turbulence in the flow at a tidal stream power site. *Philos Trans A Math Phys Eng Sci.* 2013 Jan 14;371(1985):20120196. doi: 10.1098/rsta.2012.0196. Print 2013 Feb 28.

Pelli, D., Cappietti, L., Oumeraci, H., 2016. Assessing the wave energy potential in the Mediterranean Sea using WAVEWATCH III. *Proceedings of Renew 2016, 2nd International Conference on Renewable Energies Offshore*, October 2016.

Vicinanza, D., Cappietti, L., Contestabile, P., 2009. Assessment of Wave Energy around Italy. *Proceedings of the 8th European Wave and Tidal Energy Conference, Uppsala, Sweden*, 2009.

Walker, S., Cappietti, L., Experimental Studies of Turbulent Intensity around a Tidal Turbine Support Structure, *Energies*, 2017, 10, 497.

Walker, S., Cappietti, L., Simonetti, I. A laboratory study on the effects of waves on the performance and structural deflection of a tidal stream turbine, *13th European Wave and Tidal Energy Conference (EWTEC)*, September 2019, Naples.